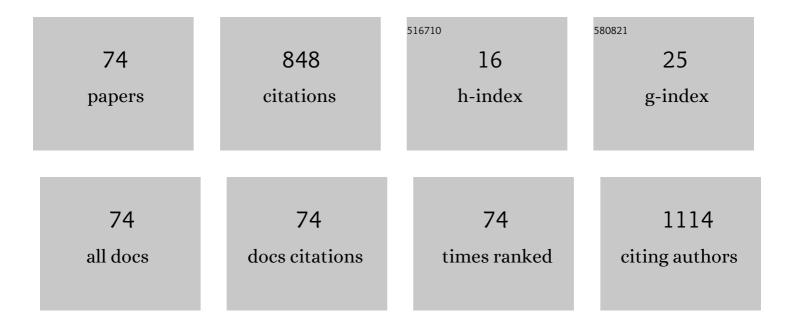
List of Publications by Year in descending order

Source: https://exaly.com/author-pdf/5157892/publications.pdf Version: 2024-02-01



#	Article	IF	CITATIONS
1	Statistical metal–insulator transition properties of electric domains in NdNiO ₃ nanowires. Japanese Journal of Applied Physics, 2022, 61, SM1005.	1.5	0
2	Controllable Strongly Electron-Correlated Properties of NdNiO ₃ Induced by Large-Area Protonation with Metal–Acid Treatment. ACS Applied Electronic Materials, 2022, 4, 3495-3502.	4.3	5
3	Realization of Non-degrading Huge Resistance Changes in the Metal Oxide Nanostructures Utilizing the Perfect Crystal Growth Techniques. Vacuum and Surface Science, 2022, 65, 321-326.	0.1	Ο
4	Nanofabrication and Physical Properties Investigation on the Three-dimensional Surfaces =Diversity and Inclusion in Surface Science=. Vacuum and Surface Science, 2021, 64, 126-133.	0.1	1
5	Spatial Analytical Surface Structure Mapping for Three-dimensional Micro-shaped Si by Micro-beam Reflection High-energy Electron Diffraction. E-Journal of Surface Science and Nanotechnology, 2021, 19, 13-19.	0.4	3
6	Realization of the three-dimensionally architected nanostructures for the strongly electron correlated metal oxides and investigation of their nanoscale metal-insulator transition properties. Journal of the Society of Japanese Women Scientists, 2021, 21, 13-21.	0.0	0
7	Atomically Architected Silicon Pyramid Single-Crystalline Structure Supporting Epitaxial Material Growth and Characteristic Magnetism. Crystal Growth and Design, 2021, 21, 946-953.	3.0	2
8	Nondeteriorating Verwey Transition in 50 nm Thick Fe ₃ O ₄ Films by Virtue of Atomically Flattened MgO Substrates: Implications for Magnetoresistive Devices. ACS Applied Nano Materials, 2021, 4, 12091-12097.	5.0	4
9	Prominent Verway Transition of Fe3O4 Thin Films Grown on Transferable Hexagonal Boron Nitride. ACS Applied Electronic Materials, 2021, 3, 5031-5036.	4.3	2
10	Catalytic Hydrogen Doping of NdNiO ₃ Thin Films under Electric Fields. ACS Applied Materials & Interfaces, 2020, 12, 54955-54962.	8.0	15
11	Creation and Evaluation of Atomically Ordered Side- and Facet-Surface Structures of Three-Dimensional Silicon Nano-Architectures. , 2020, , .		1
12	Investigation of Statistical Metal-Insulator Transition Properties of Electronic Domains in Spatially Confined VO2 Nanostructure. Crystals, 2020, 10, 631.	2.2	14
13	Ultrafast reflectivity change of vanadium dioxide induced by THz field enhanced by a metallic structure. Japanese Journal of Applied Physics, 2019, 58, 083002.	1.5	1
14	Three-Dimensional Nanoconfinement Supports Verwey Transition in Fe ₃ O ₄ Nanowire at 10 nm Length Scale. Nano Letters, 2019, 19, 5003-5010.	9.1	14
15	Barrier Formation at the Contacts of Vanadium Dioxide and Transition-Metal Dichalcogenides. ACS Applied Materials & Interfaces, 2019, 11, 36871-36879.	8.0	9
16	Effects of Off-Stoichiometry in the Epitaxial NdNiO ₃ Film on the Suppression of Its Metal-Insulator-Transition Properties. ACS Applied Electronic Materials, 2019, 1, 2678-2683.	4.3	13
17	Correlation between Ni Valence and Resistance Modulation on a SmNiO3 Chemical Transistor. ACS Applied Electronic Materials, 2019, 1, 82-87.	4.3	11
18	Gate-Tunable Thermal Metal–Insulator Transition in VO ₂ Monolithically Integrated into a WSe ₂ Field-Effect Transistor. ACS Applied Materials & Interfaces, 2019, 11, 3224-3230.	8.0	29

#	Article	IF	CITATIONS
19	Shape-fitting analyses of two-dimensional X-ray diffraction spots for strain-distribution evaluation in a β-FeSi ₂ nanofilm. Journal of Applied Crystallography, 2019, 52, 732-744.	4.5	1
20	Non-contact detection of nanoscale structures using optical nanofiber. Optics Express, 2019, 27, 367.	3.4	0
21	Wide-Range Resistance Modulation on a SmNiO3 Chemical Transistor. ECS Meeting Abstracts, 2019, , .	0.0	0
22	Electric transport properties for three-dimensional angular-interconnects of Au wires crossing facet edges of atomically-flat Si{111} surfaces. Japanese Journal of Applied Physics, 2018, 57, 090303.	1.5	5
23	Fabrication of the electric double layer transistor with (La,Pr,Ca)MnO3 nanowall wire channel. Modern Physics Letters B, 2018, 32, 1840058.	1.9	2
24	Arrangement of self-assembled ZnO-NiO nanostructures using topographical templates towards oxide directed self-assembly. AIP Advances, 2018, 8, 115029.	1.3	2
25	Strongly correlated perovskite lithium ion shuttles. Proceedings of the National Academy of Sciences of the United States of America, 2018, 115, 9672-9677.	7.1	55
26	Epitaxial crystallization of self-assembled ZnO–NiO nanopillar system. Applied Physics Express, 2017, 10, 075501.	2.4	4
27	Direct observation for atomically flat and ordered vertical {111} side-surfaces on three-dimensionally figured Si(110) substrate using scanning tunneling microscopy. Japanese Journal of Applied Physics, 2017, 56, 111301.	1.5	8
28	Enhancement of discrete changes in resistance in engineered VO ₂ heterointerface nanowall wire. Applied Physics Express, 2017, 10, 115001.	2.4	8
29	Monitoring Thermally Induced Cylindrical Microphase Separation of Polystyrene- <i>block</i> -poly(methyl methacrylate) by Atomic Force Microscopy. Journal of Photopolymer Science and Technology = [Fotoporima Konwakai Shi], 2016, 29, 659-665.	0.3	0
30	Methods of creating and observing atomically reconstructed vertical Si{100}, {110}, and {111} side-surfaces. Applied Physics Express, 2016, 9, 085501.	2.4	8
31	Molecule desorption induced by gate-voltage application in MOS structure. Applied Physics Express, 2016, 9, 047002.	2.4	Ο
32	Creation of atomically flat Si{111}7 × 7 side-surfaces on a three-dimensionally-architected Si(110) substrate. Surface Science, 2016, 644, 86-90.	1.9	10
33	3D-Architected and Integrated Metal Oxide Nanostructures and Beyond Produced by Three-Dimensional Nanotemplate Pulsed Laser Deposition. E-Journal of Surface Science and Nanotechnology, 2015, 13, 279-283.	0.4	10
34	Identification of Giant Mott Phase Transition of Single Electric Nanodomain in Manganite Nanowall Wire. Nano Letters, 2015, 15, 4322-4328.	9.1	19
35	Discrimination between gate-induced electrostatic and electrochemical characteristics in insulator-to-metal transition of manganite thin films. Applied Physics Express, 2015, 8, 073201.	2.4	6
36	Selection of Di(meth)acrylate Monomers for Low Pollution of Fluorinated Mold Surfaces in Ultraviolet Nanoimprint Lithography. Langmuir, 2015, 31, 4188-4195.	3.5	21

#	Article	IF	CITATIONS
37	Local atomic configuration of graphene, buffer layer, and precursor layer on SiC(0001) by photoelectron diffraction. Surface Science, 2015, 632, 98-102.	1.9	7
38	Functional metal oxide nanostructures fabricated by 3D-nanotemplate PLD. , 2014, , .		0
39	Systematic study of surface magnetism in Si(111)–Fe system grown by solid phase epitaxy: In situ schematic magnetic phase diagram of Si(111)–Fe. Journal of Magnetism and Magnetic Materials, 2014, 363, 158-165.	2.3	6
40	MoS ₂ Nanocube Structures as Catalysts for Electrochemical H ₂ Evolution from Acidic Aqueous Solutions. ACS Applied Materials & Interfaces, 2014, 6, 2003-2010.	8.0	51
41	Artificial three dimensional oxide nanostructures for high performance correlated oxide nanoelectronics. Japanese Journal of Applied Physics, 2014, 53, 05FA10.	1.5	6
42	Fabrication of three-dimensional epitaxial (Fe,Zn) ₃ O ₄ nanowall wire structures and their transport properties. Applied Physics Express, 2014, 7, 045201.	2.4	14
43	Enhancement of photoluminescence efficiency from GaN(0001) by surface treatments. Japanese Journal of Applied Physics, 2014, 53, 021001.	1.5	9
44	Ni and p-Cu2O Nanocubes with a Small Size Distribution by Templated Electrodeposition and Their Characterization by Photocurrent Measurement. ACS Applied Materials & Interfaces, 2013, 5, 10938-10945.	8.0	9
45	Epitaxial inversion on ferromagnetic (Fe,Zn)3O4 /ferroelectric BiFeO3 core-shell nanodot arrays using three dimensional nano-seeding assembly. Journal of Applied Physics, 2013, 113, .	2.5	12
46	Nanowall-Shaped MgO Substrate with Flat (100) Sidesurface: A New Route to Three-Dimensional Functional Oxide Nanostructured Electronics. Japanese Journal of Applied Physics, 2013, 52, 015001.	1.5	20
47	In-Plane Oblique Pulsed-Laser Deposition and Its Application to the Fabrication of Metal Oxide Nanoconstrictions. Applied Physics Express, 2013, 6, 035201.	2.4	5
48	Controlled fabrication of artificial ferromagnetic (Fe,Mn) ₃ O ₄ nanowall-wires by a three-dimensional nanotemplate pulsed laser deposition method. Nanotechnology, 2012, 23, 485308.	2.6	16
49	Self-Assembled Growth of Spinel (Fe,Zn)\$_{3}\$O\$_{4}\$–Perovskite BiFeO\$_{3}\$ Nanocomposite Structures Using Pulsed Laser Deposition. Japanese Journal of Applied Physics, 2012, 51, 035504.	1.5	4
50	ZnO Nanobox Luminescent Source Fabricated by Three-Dimensional Nanotemplate Pulsed-Laser Deposition. Applied Physics Express, 2012, 5, 125203.	2.4	15
51	Atomically Smooth Gallium Nitride Surfaces Prepared by Chemical Etching with Platinum Catalyst in Water. Journal of the Electrochemical Society, 2012, 159, H417-H420.	2.9	36
52	Structural and chemical characteristics of atomically smooth GaN surfaces prepared by abrasive-free polishing with Pt catalyst. Journal of Crystal Growth, 2012, 349, 83-88.	1.5	32
53	Position-controlled functional oxide lateral heterostructures consisting of artificially aligned (Fe,Zn)3O4nanodots and BiFeO3matrix. Nanotechnology, 2012, 23, 335302.	2.6	8
54	Structure and Magnetic Properties of Mono- and Bi-Layer Graphene Films on Ultraprecision Figured 4H-SiC(0001) Surfaces. Journal of Nanoscience and Nanotechnology, 2011, 11, 2897-2902.	0.9	0

#	Article	IF	CITATIONS
55	Dependence of Process Characteristics on Atomic-Step Density in Catalyst-Referred Etching of 4H–SiC(0001) Surface. Journal of Nanoscience and Nanotechnology, 2011, 11, 2928-2930.	0.9	30
56	Improved Optical and Electrical Characteristics of Free-Standing GaN Substrates by Chemical Polishing Utilizing Photo-Electrochemical Method. Journal of Nanoscience and Nanotechnology, 2011, 11, 2882-2885.	0.9	3
57	Formation of wide and atomically flat graphene layers on ultraprecision-figured 4H-SiC(0001) surfaces. Surface Science, 2011, 605, 597-605.	1.9	26
58	Position-, size-, and shape-controlled highly crystalline ZnO nanostructures. Nanotechnology, 2011, 22, 415301.	2.6	23
59	Identifying valence band structure of transient phase in VO2thin film by hard x-ray photoemission. Physical Review B, 2011, 84, .	3.2	21
60	Graphene Formation on 4H-SiC(0001) Surface Flattened by Catalyst-Assisted Chemical Etching in HF Solution. ECS Transactions, 2011, 41, 241-248.	0.5	0
61	Damage-Free Dry Polishing of 4H-SiC Combined with Atmospheric-Pressure Water Vapor Plasma Oxidation. Japanese Journal of Applied Physics, 2011, 50, 08JG05.	1.5	9
62	Abrasive-Free Planarization of 3-Inch 4H-SiC Substrate Using Catalyst-Referred Etching. Materials Science Forum, 2011, 679-680, 493-495.	0.3	3
63	Efficient Wet Etching of GaN (0001) Substrate with Subsurface Damage Layer. Journal of Nanoscience and Nanotechnology, 2011, 11, 2979-2982.	0.9	2
64	Damage-Free Dry Polishing of 4H-SiC Combined with Atmospheric-Pressure Water Vapor Plasma Oxidation. Japanese Journal of Applied Physics, 2011, 50, 08JG05.	1.5	12
65	Chemical etchant dependence of surface structure and morphology on GaN(0001) substrates. Surface Science, 2010, 604, 1247-1253.	1.9	33
66	Surface treatments toward obtaining clean GaN(0001) from commercial hydride vapor phase epitaxy and metal-organic chemical vapor deposition substrates in ultrahigh vacuum. Applied Surface Science, 2010, 256, 4745-4756.	6.1	51
67	High-Integrity Finishing of 4H-SiC (0001) by Plasma-Assisted Polishing. Advanced Materials Research, 2010, 126-128, 423-428.	0.3	27
68	Planarization of GaN(0001) Surface by Photo-Electrochemical Method with Solid Acidic or Basic Catalyst. Japanese Journal of Applied Physics, 2009, 48, 121001.	1.5	16
69	Interface Structure of an Epitaxial Iron Silicide on Si(111) Studied with X-Ray Diffraction. E-Journal of Surface Science and Nanotechnology, 2009, 7, 513-517.	0.4	5
70	Xâ€ray photoelectron spectroscopy of SPEâ€grown bccâ€Fe, polycrystal and βâ€FeSi ₂ phases on Si(111) surfaces. Surface and Interface Analysis, 2008, 40, 988-992.	1.8	5
71	Formation of ferromagnetic interface between β-FeSi2 and Si(111) substrate. Applied Physics Letters, 2007, 91, 201916.	3.3	22
72	Total analysis of surface structure and properties by UHV transfer system. Surface Science, 2007, 601, 5284-5288.	1.9	13

#	Article	IF	CITATIONS
73	Atomic structure of Fe thin-films on Cu(0 0 1) studied with stereoscopic photography. Applied Surface Science, 2004, 237, 311-315.	6.1	6
74	Influence of the UV Light Intensity on the Photoelectrochemical Planarization Technique for Gallium Nitride. Materials Science Forum, 0, 645-648, 795-798.	0.3	8